Advances in Intelligent Systems Research, volume 165

International Conference on Modeling, Simulation, Optimization and Numerical Techniques (SMONT 2019)

The Study of Motion Analysis and Control Principle of Three-DOF Turnover Wall

Shiwen Zhao[1],Tianyu Wu[1], Wensheng Xu[1,2,*], Xiaoxiang Jiang[1,2], Xuefeng Li[1], Qianrong Wang[1] and Weifeng Kang[1]

[1]Engineering Laboratory for Energy System Process Conversion & Emission Control Technology of Jiangsu Province, School of Energy & Mechanical Engineering, Nanjing Normal University, Nanjing 210042, China

[2]Key Laboratory of Biomass Energy and Material of Jiangsu Province, Nanjing 210042, China

[*]Corresponding author

***Abstract*—A three-DOF(degree of freedom) parallel mechanism is designed and integrated with the moveable wall which the solar photovoltaic panels are installed on it. In order to control the spatial posture of the wall, geometric analysis was used to get the kinematic inverse solution and the kinematic positive solution of the mechanism, to obtain the relationship among push distance, rotation angle and flip angle. MATLAB was used to get numerical solution and show the relationship of them intuitively. The motor control program was designed and optimized through feedback structure. The motor could be controlled according to the deviation. Result indicates the wall can be controlled more accurately according to the change of solar angle and gets the maxmal generating efficiency.**

Keywords—prefabricated building; parallel mechanism; positive and inversion solution analysis; solar energy

I. INTRODUCTION

Parallel mechanism is widely used because of the good dynamic performance [1]. It can be found in many applications, such as airplane simulators, adjustable articulated trusses and mining machines. J. Wang et al [2] derived the velocity equations and the singularity loci of the three types of kinematically redundant parallel mechanisms they proposed. It should be acknowledged that the kinematically redundant machanisms have improved performance over non-redundant ones [3,4]. Moreover, O.Altuzarra et al. have been researching on parallel continuum mechanisms. They did quasistatic analysis [5,6], used numerical direct integration to looking for possible solutions, and then made use of particular conditions on a certain mechanism to find systematically all solutions [7,8]. As for the control of the mechanisms, cable-driven parallel mechanisms are widely used [9,10,11], however, the interference between cables that may occur during movement [12,13].

In order to make full use of buliding space and solar energy in prefabricated building, a new parallel mechanism is designed and solar photovoltaic panels are installed on the moveable wall. By changing the spatial posture of the wall the objective can be achieved. In this paper, the structure is disscussed. The kinematic positive and inverse solution is analyzed, the relationship between the push distance of the electric push rods and space angle is gotten. MATLAB is used to carry out simulation analysis. Control strategy is designed to achieve more accurate control.

II. ANALYSIS OF KINEMATIC

A. Establishment of Analytical Model

Figure I(a) shows the multi-degree-of-freedom reversing mechanism which is turnover and can be circularly assembled. The wall is open-close and its structure is shown in Figure I(b). In the mechanism, three electric push rods are connected to the turnover outer wall through the fish eyeball universal join. The wall cannot rotate around the top of the electric push rod or move horizontally along both sides of the rod because of the restriction of the fish eyeball universal joint with locating pin at the top. With the cooperation of the three electric push rods, the wall can change the spatial pose according to the control requirements.

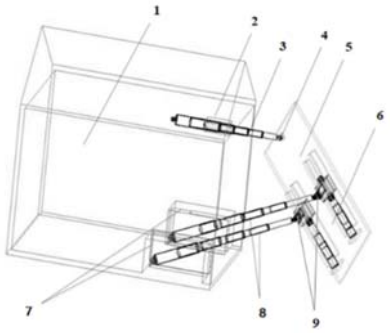

(a)

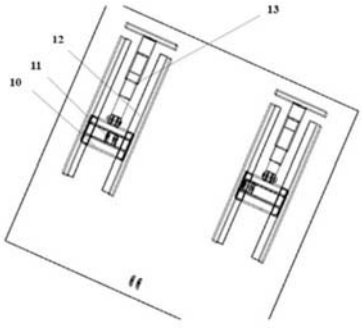

(b)

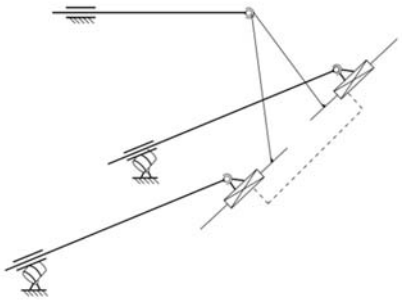

(c)

FIGURE I. THE STRUCTURE OF MECHANISM (1- FIXED WALL; 2- THE FIRST ELECTRIC PUSH ROD FIXING DEVICE; 3- THE FIRST ELECTRIC PUSH ROD; 4- FISH EYEBALL UNIVERSAL JOINT WITH LOCATING PIN; 5-FLIPPED OUTER WALL; 6- SOLAR PHOTOVOLTAIC PANEL; 7- THE SECOND ELECTRIC PUSH ROD STORAGE BOX; 8- THE SECOND ELECTRIC PUSH ROD; 9-ISH EYEBALL UNIVERSAL JOINT WITHOUT LOCATING PIN; 10- THE SLIDER; 11- THE SECONDARY SLIPPERY COURSE; 12- THE PRIOR SLIPPERY COURSE; 13- SLIDE RAIL ELECTRIC PUSH ROD)

Structural diagram of this mechanism structure is shown in Figure I(c), the calculation formula of single closed loop of space mechanism is used to get its degrees of freedom:

$$M = (6 - m)n - \sum_{k=m+1}^{k=5}(k - m)P_k = 3 \qquad (1)$$

In this formula, m represents the number of common constraint, n represents the number of component, k represents the constraint number of kinematic pair of level k, P_k represents the number of kinematic pair of level k.

From the analysis above, the wall has three degrees of freedom, namely, one degree of freedom to move along the X-axis and two degrees of freedom to rotate around A_2 points parallel to the z-axis and A_2P axis.

In the process of posture adjustment, the electric push rod receives the operation command and by adjusting the push distance, the wall can reach the required posture. For the convenience of research, the movement process is divided into three steps:

The first step is to achieve the non-interference posture. The first electric push rod motor controls the extension of the push rod outwards to make the upside of the outer wall do not interfere with the wall during the period from moving horizontally out to the flip process. The second step is to get the retroflex posture based on the first step. The two second electric push rods coordinate synchronously so that the wall takes the horizontal straight line where the first electric push rod connects the hinge point A_2 to the wall as the axis, and flips upward to the desired angle, at which point the outer wall takes an angle of θ to rearrange itself in the YOZ plane. The third step is to reach the rotating posture. Based on the retroflex posture and according to the solar elevation angles, motors control the two second electric push rods and makes the push distance of them different, thus the wall rotates to the demand angle of φ along the A_2P axis. If the demand of θ and φ changes, then the two second electric push rods adjust the push distance according to the new requirements to achieve the new order of posture; If the outer wall needs to be closed, the push distance of the three electric push rods shall be controlled to zero to reach the closed state. According to the method of calculation of Pan F[14], we defined the solar elevation angles so that the design scope of work space of the wall can be achieved theoretically at θ:(0°)-(81°), φ:(-45°)-(+45°).

The global coordinate system o-xyz was established at point O, where the hinge points installed on the ground by the two second electric push rods are B_{11} and B_{12} respectively, and the hinge points connected with the wall were B_{21} and B_{22} respectively. The projection length of the line $B_{21}B_{22}$ on the z-axis is 2d, and the perpendicular line from A_2 to the line $B_{21}B_{22}$ was made, and the vertical foot is P. The hinge point of the first electric push rod is A_1, the hinge point connecting with the wall is A_2, and the initial installation length of the three electric push rods are all S_0.

Analysis of kinematic inverse solution

Based on the analysis above, when analysis the first step of flip, the wall rotates along the horizontal axis of the hinge point A_2. The two second electric push rods synchronously push out during the rotation, so in this step, the model is simplified to the XOY two-dimensional projection plane to analyze. In Figure III, a is the distance from B_1 to the wall, b is the distance from A_1 to the bottom, c is the length of A_2B_2, the push distance of the first electric push rod is S_{t1}, the push distance of the two second electric push rods with two coupling motions is S_{t2} and S_{t3}, and the total length is S_z.

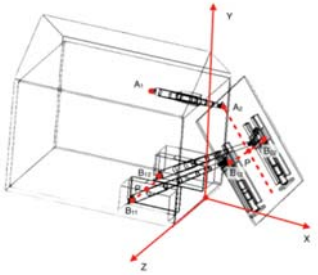

FIGURE II. FLIP STATE DIAGRAM

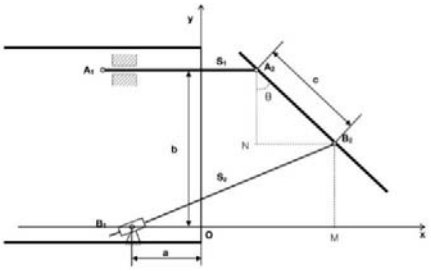

FIGURE III. XOY two-dimensional projection plane

A_2 and B_2 are hinge points and the auxiliary point N. The coordinates of B_2 are set as (X,Y,Z), then we get each vector between any two points. By using trigonometric function and analysis the geometric relationship between the points, we can get $|\overrightarrow{B_1B_2}|$ which is directly related to S_t. In conclusion, the relationship between push distance S_t of the bottom electric push rod and flip angle θ, can be obtained as St=f(θ):

$$S_{t2} = S_{t3} = \sqrt{\left(S_{t1} + \sqrt{c^2 - (-\mathrm{c}\cos\theta)^2} + a\right)^2 + (\mathrm{b} - \mathrm{c}\cos\theta)^2} - S_0 \quad (2)$$

After reaching the required reversal angle, the second step of wall movement is studied, which is analyzing the relationship between the push distance of two second electric push rods and the rotation angle of the wall. In the process of rotation, the wall rotation along the A_2P axis in Figure IV is controlled by adjusting the difference of push distance between the two rods. By analyzing the two rotational states, Figure V can be obtained according to the direction of projection. Two hinge points of the two second electric push rods connected to the wall change into B_{21}', B_{22}' from B_{21}, B_{22}.

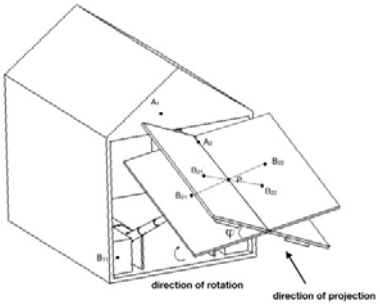

FIGURE IV. Schematic diagram of rotational state

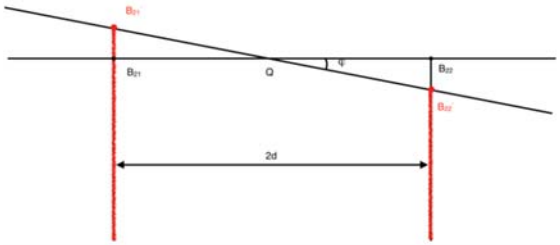

FIGURE V. Schematic diagram of the position of rotating wall

At this point, in the second step, the final relationship between the push distance of the three push electric rods and the rotation angle φ is:

$$S_{t2,t3} = \sqrt{\left(S_{t1} + \sqrt{c^2 - (-\mathrm{c}\cos\theta)^2} \pm d\tan\varphi\cos\theta + a\right)^2 + (\mathrm{b} - \mathrm{c}\cos\theta + d\tan\varphi\sin\theta)^2} - S_0. \quad (3)$$

Analysis of kinematic positive solution

The kinematic positive solution analysis of the parallel mechanism means that the input value of the push distance is known and the spatial position of the moving end need to be obtained.

In the process of changing the spatial pose, by analyzing the geometric relationship of motion posture in Figure III, it can be known that there always exists two right triangles A_2NB_2 and B_1MB_2. Then, the analytical formula of the positive kinematic solution of movement of the wall, $\theta = f(S_t)$, is obtained:

$$\theta = \arctan\left[\frac{\left(\frac{(-a^2+b^2-c^2+S_z{}^2+S_{t1}{}^2)}{2(a+S_{t1})} - \frac{b\left[a^2b-(S_{t1}+a)\sqrt{[-AB]}+C\right]}{2(a+S_{t1})(a^2+2aS_{t1}+b^2+S_{t1}{}^2)} - S_{t1}\right)}{\left(\mathrm{b} - \frac{\left[a^2b-(S_{t1}+a)\sqrt{[-AB]}+C\right]}{2\left(a^2+2aS_{t1}+b^2+S_{t1}{}^2\right)}\right)}\right] \quad (4)$$

while

$$\mathrm{A} = \left(a^2 + 2aS_{t1} + b^2 - c^2 - 2cS_z - S_z{}^2 + S_{t1}{}^2\right)$$

$$\mathrm{B} = \left(a^2 + 2aS_{t1} + b^2 - c^2 + 2cS_z - S_z{}^2 + S_{t1}{}^2\right)$$

$$\mathrm{C} = \left(-bc^2 + bS_z{}^2 + bS_{t1}{}^2 + b^3 + 2abS_{t1}\right)$$

According to this, controlling the angle of the wall's retroflex posture according to the requirements can be realized accurately by controlling the push distance of electric push rods in order to finish the first step of wall movement. During the rotating, let's set the solution for x and y to be X_1 and Y_1 respectively. Wall initial position on the projective pale is $B_{21}B_{22}$, after rotation is $B_{21}{}'B_{22}{}'$, $B_{21}B_{22}$ is always going to be 2d on the z-axis, through projection and vector relationships, the final formulas of kinematic positive solution can be expressed as:

$$\varphi = \arctan\left(\frac{\left|S_{t2} - \frac{S_{t2}+S_{t3}}{2}\right|\cos\left(\theta - \arctan\left(\frac{Y_1}{X_1+a}\right)\right)}{d}\right) \quad (5)$$

III. Experimental Simulation Analysis of Turnover Wall

The relationship between the push distance of the second electric rod and the posture angle

The spatial pose of the turnover wall is related to the size parameters, shape and installation position of the mechanism, which can reflect the mapping relationship between the posture of the end of the rods and the push distance of them. By analyzing a branched chain constraint of parallel mechanism, the relationship between the constraint and the pose angle can be obtained.

The relationship between the push distance and the angle of the second electric rod in turnover and recyclable building structure can be describe as a three-dimensional space of which the boundary is $Q(S_{t2}, \theta, \varphi) = 0$. The distance between B_1 and the wall is a=1m, A_1 is 2.8m away from the base and A_2 B_2 which is defined as c is 2m. The initial installation length of the three electric rods are all S_0=1m, the push distance of the first push rod is S_{t1}=1m, the push distance of the two second electric rods with coupling motions is S_{t2} and S_{t3}, respectively. According to the given parameter conditions and constraints, the corresponding program was written in MATLAB, and the relationship in Figure VI is obtained.

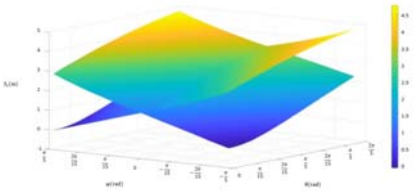

FIGURE VI. THE RELATIONSHIP BETWEEN THE PUSH DISTANCE OF THE SECOND ELECTRIC ROD AND THE POSTURE ANGLE

By analyzed Figure VI we can know that controlling the push distance of the second electric rod can accurately control the movable wall to the certain spatial pose. What's more, when given an angle of θ or φ, the push distance of the second electric push rod, which controls the movement of the turnover wall, S_{t2}, meets the nonlinear relation with the other angle.

When the rotation angle is zero, the push distance of the two second electric rods are different. As shown in Figure VI, under the control of motors having the same speed, the push distance of the two second electric rods S_t increases synchronously as their flip angle increases. When the flip angle is a constant, with the change of rotation angle, the push distance S_t of the two rods increases or decreases respectively at the same speed under the control of motors having the same speed. When the flip angle and rotation angle both change, the two motors control the electric rods at different speeds or turns, so that the push distance S_t of the two second electric push rods respectively reach the required value.

Analysis of the process of changing the spatial pose

After analyzing the relationship between the push distance of the second electric rod and the posture angle, we want to study the relationship between push distance S_{t2}, S_{t3} and flip angle θ. In Figure VI, when φ= 0 °, we study the cross section of S_t-θ and the relationship is shown in Figure VII, which expresses the relationship between the demand flip angle and the push distance when the rotation angle is 0.

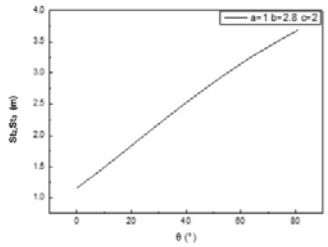

FIGURE VII. WHEN φ=0°, THE RELATIONSHIP BETWEEN S_T AND Θ

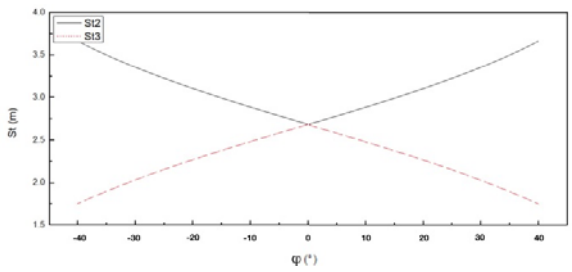

FIGURE VIII. WHEN Θ=0°, THE RELATIONSHIP BETWEEN S_T AND φ

When study the relationship between the push distance S_t and the rotation angle φ. The range of φ is -45~45°. In Figure VI, when θ= 60°, we study the cross section of S_t-φ and the relationship is shown inFigure VIII which expresses the relationship between the demand rotation angle and the push distance when the flip angle is 60°.

IV. CONTROL OPTIMIZATION

The motor is controlled by closed-loop control, that is, deviation control. By analyzing the kinematic relationship between the components and using Laplace transform, the structure block diagram of the controller is shown in Figure IX(a). Based on this, we increase the accuracy of motor control by adding feedback structure to the angular displacement of the transmission shaft, as shown in Figure IX(b). In Figure IX(c) we consider the effects of external load torque, friction torque, gravity torque and centripetal force. The combination of feedback control and external disturbance control makes the control more accurate.

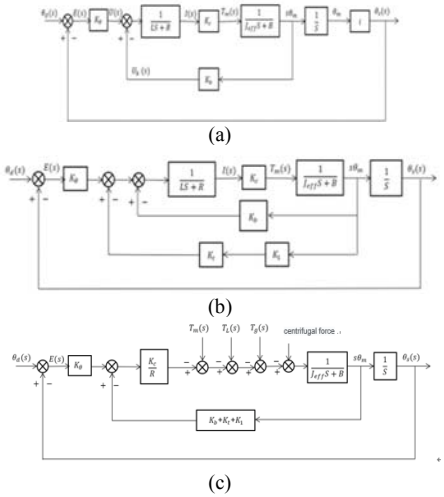

(a)

(b)

(c)

FIGURE IX. THE STRUCTURE BLOCK DIAGRAM OF THE CONTROLLER(T_M IS THE TORQUE OUTPUT BY MOTOR; T_l IS THE TOTAL TORQUE OF THE LOAD; T_Θ IS THE TORQUE OF THE ACHOMETER GENERATOR; Θ_S IS THE LOAD SHAFT ANGLE; I IS ARMATURE WINDING CURRENT; Θ_M IS THE ANGULAR DISPLACEMENT OF THE DRIVING SHAFT; K_B IS THE ELECTROMOTIVE FORCE CONSTANT OF THE MOTOR; K_C IS THE TORQUE CONSTANT OF THE MOTOR; K_Θ IS THE CONVERSION CONSTANT ; K_T IS THE CONSTANT OF THE TACHOMETER GENERATOR; K_1 IS THE FEEDBACK CONSTANT OF THE TACHOMETER GENERATOR; R IS ARMATURE RESISTANCE; L IS ARMATURE INDUCTANCE; J_{EFF} IS THE EQUIVALENT MOMENT OF INERTIA ON THE MOTOR SHAFT; B_{EFF} IS THE EQUIVALENT DAMPING COEFFICIENT ON THE MOTOR SHAFT)

V. SUMMARY

Using geometric analysis to analyze kinematic inverse solution and kinematic positive solution of turnover and recyclable building construction. By controlling the push distance of the electric push rod, two angles which can express the posture of the moving wall can be accurately controlled. Through the feedback structure of deviation control, the motor can accurately control the push rod to reach the predetermined

position to receive solar energy The energy absorbed by solar panels mounted on the turnover wall can be used to power the equipment in the building, thus enhance the utilization of solar energy.

ACKNOWLEDGEMENT

This research is based upon work supported by Laboratory Opening Fund of Key Laboratory of Biomass Energy and Material of Jiangsu Province [JSBEM201918].

REFERENCES

[1] J.-P. Merlet, Parallel Robots, Springer Science & Business Media, 2006

[2] J. Wang, C.M. Gosselin, Kinematic analysis and design of kinematically redundant parallel mechanisms, Trans.-Am. Soc. Mech. Eng. J. Mech. Des. 126(2004) 109–118

[3] R. Boudreau, S. Nokleby, Force optimization of kinematically-redundant planar parallel manipulators following a desired trajectory, Mech. Mach. Theory 56 (2012) 138–155. http://dx.doi.org/10.1016/j.mechmachtheory.2012.06.001.

[4] J.V. Fontes, M.M. da Silva, On the dynamic performance of parallel kinematic manipulators with actuation and kinematic redundancies, Mech. Mach. Theory 103 (2016) 148–166

[5] O. Altuzarra, M. Diez, J. Corral, G. Teoli, M. Ceccarelli, Kinematic analysis of a continuum parallel robot, in: P. Wenger, P. Flores (Eds.), New Trends in Mechanism and Machine Science, Springer International Publishing, Cham, 2017, pp. 173–180.

[6] O. Altuzarra, M. Diez, J. Corral, F.J. Campa, Kinematic analysis of a flexible tensegrity robot, in: B. Corves, E.-C. Lovasz, M. Hüsing, I. Maniu, C. Gruescu(Eds.), New Advances in Mechanisms, Mechanical Transmissions and Robotics, Springer International Publishing, Cham, 2017, pp.457–464.

[7] O. Altuzarra, D. Caballero, Q. Zhang, F.J. Campa, Kinematic characteristics of parallel continuum mechanisms, in: J. Lenarcic, V. Parenti-Castelli (Eds.),Advances in Robot Kinematics 2018, Springer International Publishing, Cham, 2019, pp. 293–301.

[8] O. Altuzarra, D. Caballero, J. Campa, C. Pinto, Forward and inverse kinematics in 2-dof planar parallel continuum manipulators, (To appear shortly inEuCoMeS 2018), 2018.

[9] W.Y. Ho, W. Kraus, A. Mangold, A. Pott, Haptic interaction with a cable-driven parallel robot using admittance control, in: Cable-Driven Parallel Robots, Springer, 2015, pp. 201–212.

[10] A. Fortin-Côté, P. Cardou, C. Gosselin, An admittance control scheme for haptic interfaces based on cable-driven parallel mechanisms, in: IEEE International Conference on Robotics and Automation (ICRA), 2014, pp. 819–825.

[11] M.J.D. Otis, M. Mokhtari, C.d. Tremblay, D. Laurendeau, F.M. d. Rainville, C.M. Gosselin, Hybrid Control with Multi-Contact Interactions for 6DOF Haptic Foot Platform on a Cable-Driven Locomotion Interface, in: Haptic interfaces for virtual environment and teleoperator systems, 2008, pp. 161–168.

[12] S. Perreault, P. Cardou, C. m. Gosselin, M.J.-D Otis, Analysis of the Interference-Free Constant-Orientation Workspace of Parallel Cable-Driven Manipulators, Journal of Mechanical Design, Transactions of the ASME 130 (10) (2010).

[13] J.-P. Merlet, Analysis of the influence of wires interference on the workspace of wire robots, in: On Advances in Robot Kinematics, Springer, 2004,pp. 211–218.

[14] Pan Fei, PV modules installation Parameter design based on MATLAB GUI[J]. Solar Energy, 2018, (08),50-55